JOURNAL OF BONE AND MINERAL RESEARCH
Volume 23, Number 12, 2008
Published online on August 4, 2008; doi: 10.1359/JBMR.080809

Disruption of BMP Signaling in Osteoblasts Through Type IA Receptor (BMPRIA) Increases Bone Mass*

Nobuhiro Kamiya,[1] Ling Ye,[2] Tatsuya Kobayashi,[3] Donald J Lucas,[1] Yoshiyuki Mochida,[4] Mitsuo Yamauchi,[4] Henry M Kronenberg,[3] Jian Q Feng,[2] and Yuji Mishina[5]

ABSTRACT: Bone morphogenetic proteins (BMPs) are known as ectopic bone inducers. The FDA approved BMPs (BMP2 and BMP7) for clinical use. However, direct effects of BMPs on endogenous bone metabolism are not yet well known. We conditionally disrupted BMP receptor type IA (BMPRIA) in osteoblasts during weanling and adult stages to show the impact of BMP signaling on endogenous bone modeling and remodeling. Cre recombination was detected in immature osteoblasts in the periosteum, osteoblasts, and osteocytes but not in chondrocytes and osteoclasts after tamoxifen administration. *Bmpr1a* conditional knockout mice (cKO) showed increased bone mass primarily in trabecular bone at P21 and 22 wk as determined by H&E staining. Vertebrae, tails, and ribs showed increased radiodensity at 22 wk, consistent with a significant increase in BMD. Both μCT and histomorphometry showed an increase in trabecular BV/TV and thickness of cKO adult bones, whereas osteoclast number, bone formation rate, and mineral apposition rate were decreased. Expression levels of bone formation markers (*Runx2* and *Bsp*), resorption markers (*Mmp9*, *Ctsk*, and *Tracp*), and *Rankl* were decreased, and *Opg* was increased in adult bones, resulting in a reduction in the ratio of *Rankl* to *osteoprotegerin* (*Opg*). The reduction in osteoclastogenesis through the RANKL–OPG pathway was also observed in weanling stages and reproduced in newborn calvaria culture. These results suggest that *Bmpr1a* cKO increased endogenous bone mass primarily in trabecular bone with decreased osteoclastogenesis through the RANKL–OPG pathway. We conclude that BMPRIA signaling in osteoblasts affects both bone formation and resorption to reduce endogenous bone mass in vivo.
J Bone Miner Res 2008;23:2007–2017. Published online on August 4, 2008; doi: 10.1359/JBMR.080809

Key words: bone morphogenetic protein, knockout, modeling and remodeling, osteoblasts, rodent

INTRODUCTION

BONE MORPHOGENETIC PROTEINS (BMPs) are members of the TGF-β superfamily and were originally discovered as ectopic bone inducers in soft tissue.[1] The osteogenic function of BMPs has been extensively examined, mainly using osteoblasts in culture.[2] The FDA approved some BMPs (BMP2 and BMP7) for clinical use in long bone open fractures, nonunions fractures, and spinal fusion. However, despite significant evidence of their potential for bone regeneration in animal and preclinical studies, the current clinical data supporting their effectiveness are not robust.[3,4] This may be because in part of a lack of understanding of the variable effects BMPs have in vivo on different cell types including chondrocytes, osteoblasts, and osteocytes.

BMP2, BMP4, and their potent receptor BMP receptor type IA (BMPRIA or ALK3) are abundantly expressed in the skeleton; however, conventional knockout (KO) mice for these genes cause early embryonic lethality.[5–7] We previously rescued the lethality of loss of *Bmpr1a* using the Cre-*lox*P system under the control of an osteocalcin promoter[8] and found that bone mass (BV/TV) evaluated by bone histomorphometry was reduced in the mutant mice at 3 mo but was increased at 10 mo. This evidence suggests that BMPs have diverse effects on bone mass, bone formation, and homeostasis in an age-dependent manner.

To understand age-dependent functions of BMP signaling in the skeleton, it is important to disrupt BMP signaling at different ages in an osteoblast-specific manner. Here, we used a tamoxifen (TM)-inducible Cre-*lox*P system under the control of a 3.2-kb type I collagen promoter (*Col1-CreER*^{TM} mice), which is activated in osteoblasts, odontoblasts, and tendon fibroblasts,[9] and disrupted BMP signaling through BMPRIA in bone. This system allows us to control the onset of the disruption of *Bmpr1a* in osteoblasts at any age by administration of TM. Because peak bone mass in the mouse is achieved after 20 wk,[10] we first focused on bone remodeling and analyzed 22-wk mice, starting TM administration at 8 wk. Moreover, to identify age-

*Parts of the manuscript were presented at the 28th Annual Meeting of the American Society for Bone and Mineral Research, Philadelphia, PA, USA, September 15–19, 2006.

The authors state that they have no conflicts of interest.

[1]Laboratory of Reproductive and Developmental Toxicology, National Institute of Environmental Health Sciences, National Institutes of Health, Research Triangle Park, North Carolina, USA; [2]Oral Biology, School of Dentistry, University of Missouri-Kansas City, Kansas City, Missouri, USA; [3]Endocrine Unit, Massachusetts General Hospital and Harvard Medical School, Boston, Massachusetts, USA; [4]Dental Research Center, University of North Carolina at Chapel Hill, Chapel Hill, North Carolina, USA; [5]University of Michigan, School of Dentistry, Ann Arbor, Michigan, USA.

dependent effects of BMP signaling, we also studied bone modeling using weanling mice starting TM administration at postnatal day 2 (P2).

In this study, we found that bone mass was increased by loss of BMP signaling in osteoblasts through BMPRIA during both stages. Osteoclastogenesis was reduced through the RANKL–osteoprotegerin (OPG) pathway, even though bone formation markers were reduced or unchanged in the mutant mice, resulting in a net increase in bone mass. This evidence suggests that BMP signaling in osteoblasts restrains endogenous bone mass, which is unexpected and contrary to the current understanding of BMPs as bone inducers.[1]

MATERIALS AND METHODS

Mice and TM administration

Mice expressing the TM-inducible Cre fusion protein Cre-ER^{TM}[11,12] under the control of a 3.2-kb mouse procollagen *α1(I)* promoter[9] (*Col1-CreER^{TM}*) were generated by pronuclear injection and crossed with floxed *Bmpr1a* mice.[13] *ROSA26* Cre reporter (*R26R*) mice were kindly provided by Dr Philippe Soriano.[14] *Col1-CreER^{TM}* mice were crossed with floxed *Bmpr1a* mice[13] to generate mice genotyped as *Col1-CreER^{TM+}*:*Bmpr1a*fx/fx and *Col1-CreER^{TM-}*:*Bmpr1a*fx/fx. TM (T5648; Sigma) was dissolved in a small volume of ethanol, diluted with corn oil at a concentration of 10 mg/ml, and stored at –20°C until use. After TM administration, Cre recombination was induced in *Bmpr1a* cKO mice (*Col1-CreER^{TM+}*:*Bmpr1a*fx/fx) but not in littermate controls (*Col1-CreER^{TM-}*:*Bmpr1a*fx/fx). In weanling mice, TM (75 mg/kg) was injected intraperitoneally into nursing females every 3 days from P2 until dissection at P14 or P21 (Fig. 1B). For adult stages, TM was injected intraperitoneally twice a week from 8 wk until dissection at 10–12 or 22 wk (Fig. 1C). Results were analyzed by comparing *Bmpr1a* cKO (*Col1-CreER^{TM+}*, *Bmpr1a*fx/fx) and littermate controls (*Col1-CreER^{TM-}*, *Bmpr1a*fx/fx), both of which received TM. No side effects on bone morphology were observed using this TM regimen. The animal protocol was approved by the Institutional Animal Care and Use Committee at the National Institute of Environmental Health Sciences, NIH.

Histology

For H&E staining, femora, tibia, humerus, tails, lumbar vertebrae, ribs, and calvaria from P21 and 22-wk mice were fixed in 4% paraformaldehyde, decalcified with 10% EDTA, and embedded in paraffin. Paraffin sections were cut in sagittal and coronal planes at 8 μm. Immunostaining was performed using rabbit polyclonal antibodies against BMPRIA[15] (1:50; Orbigen). Subsequently, an ABC kit (Santa Cruz Biotechnology) and DAB exposure were used for detection. For β-galactosidase (β-gal) staining, decalcified bones were prepared in 30% sucrose before frozen sectioning. Sections were stained with X-gal for β-gal activity and counterstained with eosin.

Static and dynamic bone histomorphometry

Adult mice received calcein (10 mg/g; Sigma) in 2% $NaHCO_3$ intraperitoneally 7 days before death at 22 wk and xylenol orange (90 mg/kg; Sigma) intraperitoneally 2 days before death. Femora and vertebrae (L_2 and L_3) were dissected and fixed in 4% paraformaldehyde. The undecalcified distal femora and vertebrae were dehydrated and embedded in methyl methacrylate. Five-millimeter longitudinal sagittal and coronal sections were cut on a Polycut S microtome (Reichert-Jung). Sections were taken from the middle of the femora, and vertebrae were stained with modified Masson's trichrome. Histomorphometric measurements were made in a blinded, nonbiased manner using the OsteoMeasure computerized image analysis system (OsteoMetrics) interfaced with an Optiphot Nikon microscope (Nikon) at a magnification of ×20. All femoral measurements were confined to the secondary spongiosa and restricted to an area between 400 and 2000 μm distal to the growth plate–metaphyseal junction of the distal femur.

For TRACP staining, decalcified lumbar (L_3) 5-μm paraffin sections were prepared as described for H&E staining. Sections were stained using the leukocyte acid phosphatase kit (Sigma) and counterstained with hematoxylin. Osteoclasts were identified as multinucleated, TRACP$^+$ cells lining the trabeculae. All measurements were made as described for bone histomorphometry.

X-ray, μCT, and DXA analyses

X-ray images of P21 and 22-wk mice were taken using Faxitron X-ray system (Faxitron X-Ray). Femora and vertebrae (L_3) were scanned using a μCT (Scanco Medical) system at 12 μm of thickness, 55 kV of energy, and 145 μA of intensity. The data were reconstructed to produce 2D and 3D images. BMD was determined by DXA using the Lunar PIXImus2 densitometer (GE).

Quantitative real-time RT-PCR

RNA was isolated from ribs and femora from weanling mice (P14 and P21) and femora and lumbar vertebrae from adult mice (10–12 wk) using the MicroFastTrack 2.0 Kit (Invitrogen). cDNA was synthesized using the SuperScript Preamplification System (Invitrogen). PCR reactions, data quantification, and analysis were performed according to the manufacturer's protocol (Applied Biosystems). Taqman primers and probes used in this study were as follows: *Bmpr1a*, Mm00477650_m1 (64 bp); runt-related transcription factor 2 (*Runx2*), Mm00501578_m1 (115 bp); osterix (*Sp7*), Mm00504574_m1 (137 bp); bone sialoprotein (*Bsp*), Mm00492555_m1 (98 bp); alkaline phosphatase (*Akp2*), Mm00475831_m1 (141 bp); osteocalcin (*Bglap2*), Mm01741771_g1 (77 bp); metalloproteinase-9 (*Mmp9*), Mm00600163_m1 (107 bp); cathepsin K (*Ctsk*), Mm00484036_m1 (84 bp); TRACP (*Tracp*), Mm00475698_m1 (79 bp); RANKL (*Rankl*), Mm00441908_m1 (69 bp); osteoprotegerin (*Opg*), Mm00435452_m1 (119 bp). Values were normalized to *Gapdh* using TaqMan Rodent GAPDH Control Reagents (Applied Biosystems). All measurements were performed in triplicate and analyzed using the $2^{-\Delta\Delta Ct}$ method.[16]

Ex vivo culture of calvarial bone

Untreated cKO calvaria were collected from newborn mice (*Cre$^+$*, *Bmpr1afx/fx*), bisected at the sagittal suture,

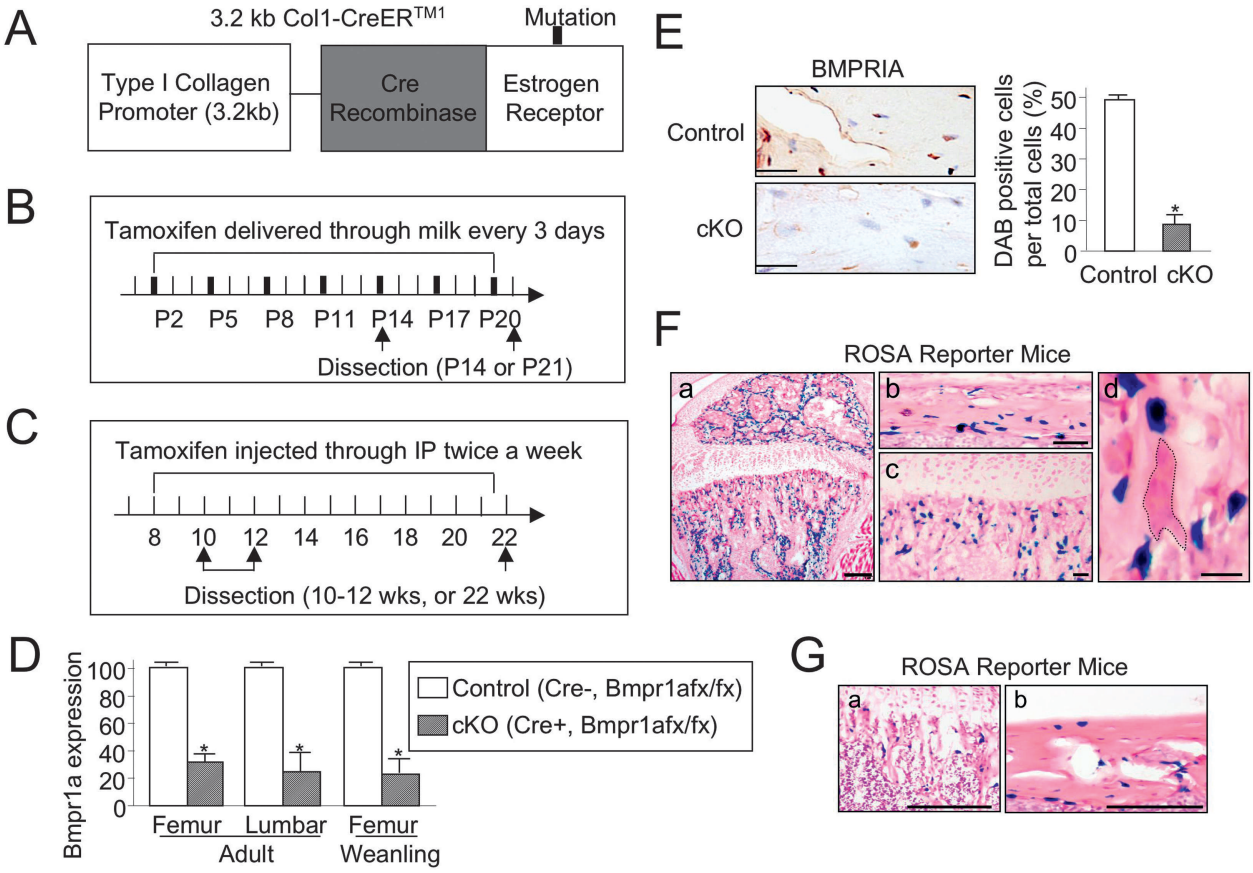

FIG. 1. *Col1-CreER^{TM}* transgenic mice. (A) TM-inducible Cre fusion protein Cre-ER^{TM} under the control of a 3.2-kb mouse procollagen $\alpha 1(I)$ promoter (*Col1-CreER^{TM}*). (B) TM administration schedule during weanling (P21) stage. TM was injected intraperitoneally into nursing females from P2 to P20 every 3 days. Both control mice (Cre^{-}, *Bmpr1a*fx/fx) and cKO mice (Cre^{+}, *Bmpr1a*fx/fx) received TM. (C) TM administration schedule during adult (22 wk) stage. TM was injected intraperitoneally into adults from 8 to 22 wk, twice a week. Both controls and cKO received TM. (D) Quantitative real-time RT-PCR shows reduced expression of *Bmpr1a* in femora and lumbar vertebrae from 10- to 12-wk mice and femora and ribs from P14 mice after recombination. *Statistically significant difference between cKO and control from three independent experiments (mean ± SD, *t*-test; *$p < 0.01$). Similar results were obtained from femora at P21. (E) BMPRIA protein in femora from 10- to 12-wk mice assessed using rabbit polyclonal antibodies against BMPRIA exposed with DAB (brown). Nuclei were stained with hematoxylin. DAB^{+} cells per total cells are shown. *Statistically significant difference between cKO (8%) and control (48%) in pooled data from three independent experiments (mean ± SD, *t*-test; *$p < 0.01$). Similar results were obtained from lumbar vertebrae at the same stage and femur at P21. Bars, 50 μm. (F) *ROSA26* Cre reporter mice showed Cre activity in osteoblasts but not in chondrocytes at P21. Cre-dependent DNA recombination was detected by β-galactosidase (β-gal) staining (a). Cortical bone (b) and trabecular bone (c) are shown. Osteoclasts were negative for β-gal (d). Bars: 1 mm (a), 50 μm (b and c), and 20 μm (d). (G) *ROSA26* Cre reporter mice showed Cre activity in osteoblasts and osteocytes in trabecular bone area (a) and cortical bone area (b) at 22 wk. Bars: 200 (a) and 100 μm (b).

and cultured in modified BGJ (Invitrogen) supplemented with ascorbic acid (50 mg/ml; Sigma) and 5% FBS (Life Technologies) for the first 24 h in culture. One hemicalvaria from each pair was treated with 4-hydroxyl (4-OH) TM (100 ng/ml; Sigma) for 5 days. The medium was changed daily.

Serum examination

Serum was collected from 22-wk-old mice. Circulating serum levels of osteocalcin (BT-470; Biomedical Technologies), pyridinoline (8019; Quidel), RANKL, and OPG (MBN-41K-1RANKL and MBN-41K-1OPG, respectively; Millipore) were measured according to the manufacturer's instructions.

Statistical analysis

All results are expressed as mean ± SD. Student's *t*-tests were used to compare data between control and cKO mice; $p < 0.05$ indicates significance.

RESULTS

Tissue specificity and efficiency of Cre recombinase in Col1-CreER^{TM} mice

Both developmental and remodeling stages are crucial for understanding bone biology. In this study, we chose two different stages, weanling (P21) and adult (22 wk), and conditionally knocked out BMP signaling through BMPRIA in

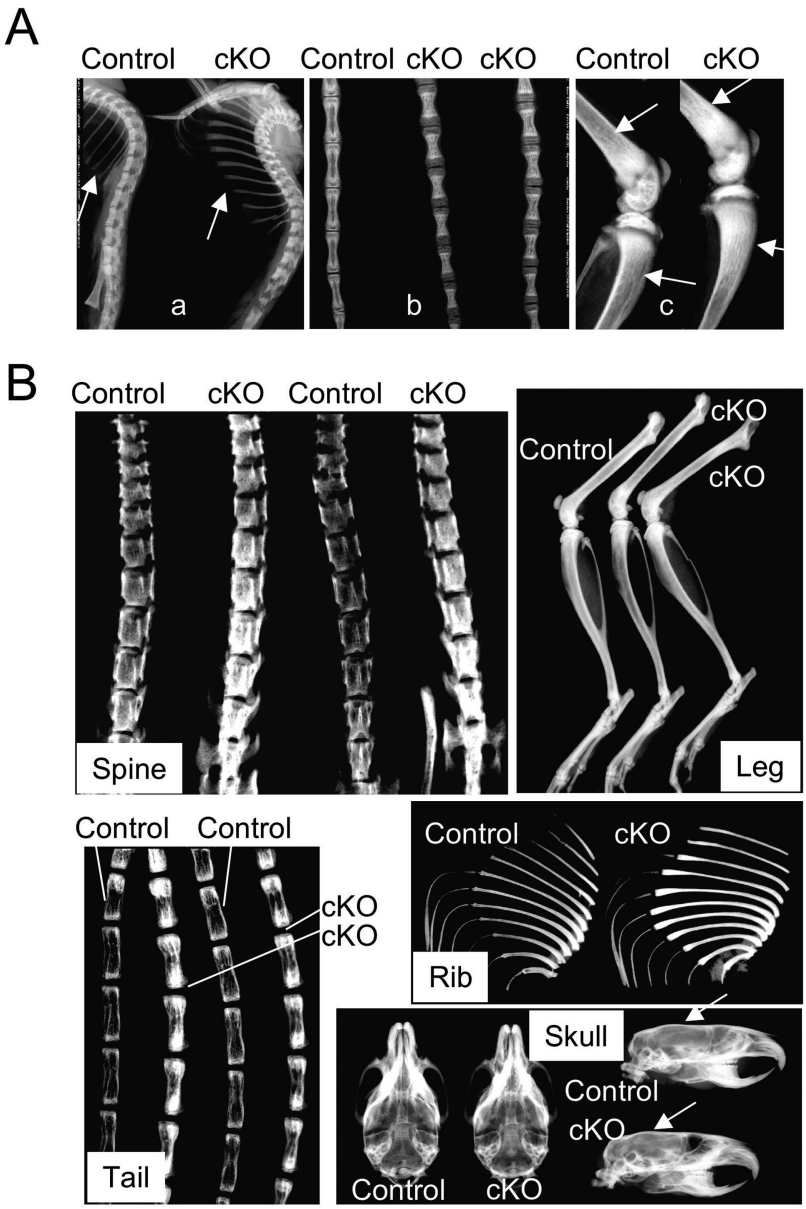

FIG. 2. Relative BMD shown by X-ray at P21 (A) and 22 wk (B). (A) White arrows indicate rib flaring (a) and increased radiodensity of metaphysis in femora (c) in P21 cKO mice. (B) Radiodensity of cKO bones was notably increased in spines, tails, and ribs but not in femora and skulls at 22 wk. White arrows indicate calvarial bones where sections were prepared (Fig. 3B, c and d).

osteoblasts using a TM-inducible Cre-*lox*P system under the control of a 3.2-kb type I collagen promoter (*Col1-CreER^{TM}*; Figs. 1A–1C).

Expression levels of *Bmpr1a* in cKO bones as determined by quantitative RT-PCR were significantly reduced >70% both in the weanling and adult stages (Fig. 1D). BMPRIA in cKO 22-wk femora decreased 84% in osteoblasts and osteocytes by immunostaining (Fig. 1E). Similar results were obtained from 22-wk lumbar vertebrae and P21 femora (data not shown). Cre efficiency and the specificity of *Col1-CreER^{TM}* expression were confirmed by β-gal staining using *R26R* mice.[14] In P21 femora, β-gal staining was observed in trabecular bone, as shown in the epiphysis and metaphysis (Fig. 1F, a), and in cortical bone (Fig. 1F, b). Staining was detected in immature periosteal cells, osteoblasts, and osteocytes (Fig. 1F, b) but not in chondrocytes (Fig. 1F, c) or soft tissues (Fig. 1F, a). Cre negative controls administered TM (*Col1-CreER^{TM-}*, $^{TM+}$) and Cre-positive mice not given TM (*Col1-CreER^{TM+}*, $^{TM-}$) showed no β-gal staining (data not shown). In addition, no Cre activity was detected in osteoclasts as shown by staining for β-gal and H&E (Fig. 1F, d). These results show that the TM administration delivered through milk specifically and efficiently disrupts BMPRIA in osteoblasts and osteocytes in weanling stages. Similarly, Cre activity was also detected in osteoblasts and osteocytes in trabecular and cortical bone at 22 wk (Fig. 1G, a and b, respectively).

Increased bone mass in Bmpr1a cKO mice

Morphologically, cKO mice appeared normal both at P21 and 22 wk with no significant difference in body weight or length compared with controls (data not shown). At P21, X-ray analyses showed rib flaring (Fig. 2A, a) and a modest

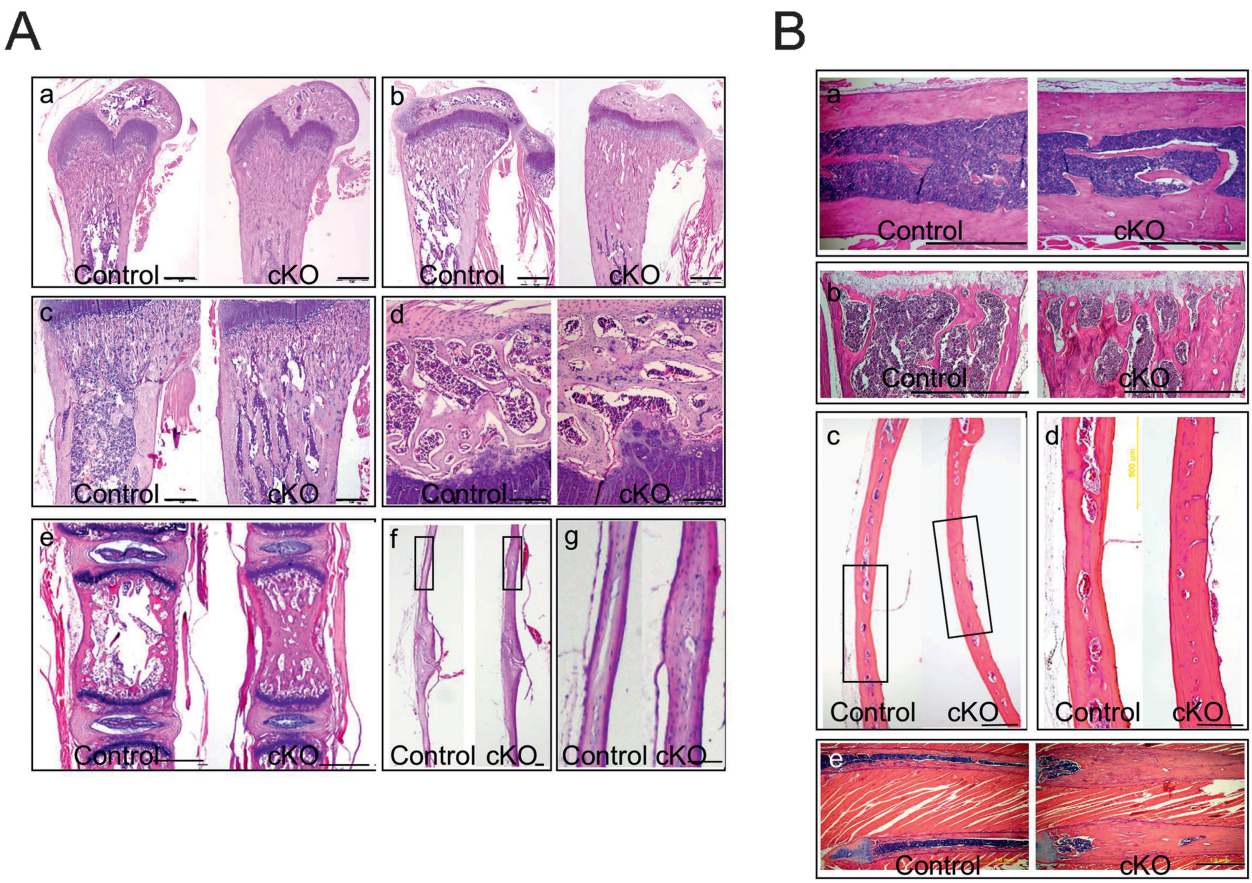

FIG. 3. Bone histology in *Bmpr1a* cKO mice at P21 (A) and 22 wk (B). (A) H&E staining of femora (a), tibia (b), humerus (c), epiphysis of humerus (d), tails (e), and calvaria (f and g). Boxes in f are magnified in g. Bone mass was increased in cKO bones. Bars: 2 mm (a, b, and e), 1 mm (c and f), 500 μm (d), and 200 μm (g). (B) H&E staining of femora cortical bone (a), lumbar (L_3) trabecular bone (b), calvaria (c and d), and ribs (e). Bone mass was increased in L_3 trabecular bone but not in femoral cortical bone. Boxes in c are magnified in d. Bars: 1 mm (a, b, and e), 500 μm (c), and 250 μm (d).

increase in radiodensity of tail trabeculae (Fig. 2A, b) and femur metaphysis (Fig. 2A, c). H&E staining showed that trabecular bone in the epiphysis and metaphysis of femur, tibia, humerus, and vertebrae (tail) were dramatically increased in cKO mice (Fig. 3A). Intramembranous calvarial bones of cKO mice were thicker than those of controls with increased woven bone (Fig. 3A, f and g). BMD measured by DXA was significantly increased in ribs (control: 0.0152 g/cm^2, cKO: 0.0163 g/cm^2; $p < 0.05$), consistent with the X-ray image (Fig. 2A, a). These results show increased bone mass in both endochondral (femur, tibia, humerus, and tail) and intramembranous (calvaria) cKO bones at P21 (Figs. 2A and 3A).

At 22 wk, rib flaring was also noted by X-ray in cKO mice (Fig. 2B) similar to P21 mice (Fig. 2A), and radiodensity in cKO bones including spine, tail, and rib cage was dramatically increased (Fig. 2B), consistent with a significant increase in BMD (Fig. 4A). H&E staining showed increased bone mass in vertebrae and ribs (Fig. 3B, b and e, respectively) where radiodensity was increased (Fig. 2B). However, the cKO femora appeared to be similar to controls by X-ray analysis (Fig. 2B), H&E staining (Fig. 3B, a), and DXA (Fig. 4A). Although cKO calvaria appeared unchanged in X-rays (Fig. 2B), H&E staining showed a smaller bone marrow cavity in cKO calvaria compared with controls (Fig. 3B, c), which probably resulted in the significant increase in BMD observed (Fig. 4A). These results show that bone mass is also increased in cKO mice during adult stages with some variation by site.

We further examined trabecular and cortical bone independently by μCT. In vertebral trabecular bone, in addition to a significant increase in tissue density (Table 1), bone volume (BV/TV) and trabecular thickness of cKO bones significantly increased 90% and 104% compared with controls, respectively (Table 1), which is shown by the 3D reconstruction (Fig. 4B). In cKO femora, tissue density of trabecular bone was significantly increased by a small amount (Table 1), suggesting that trabecular bone is increased in cKO mice to varying degrees by site. On the other hand, in cKO femoral cortical bones, there were statistically significant differences in the adult cKO femora in cortical porosity (increased), apparent density (decreased), and tissue density (decreased) as noted in Table 2. These differences are apparent in the 2D reconstruction (Fig. 4B) and by H&E staining (Fig. 3B, a). Because Cre recombination is observed in cortical bones (Fig. 1G, b), these results

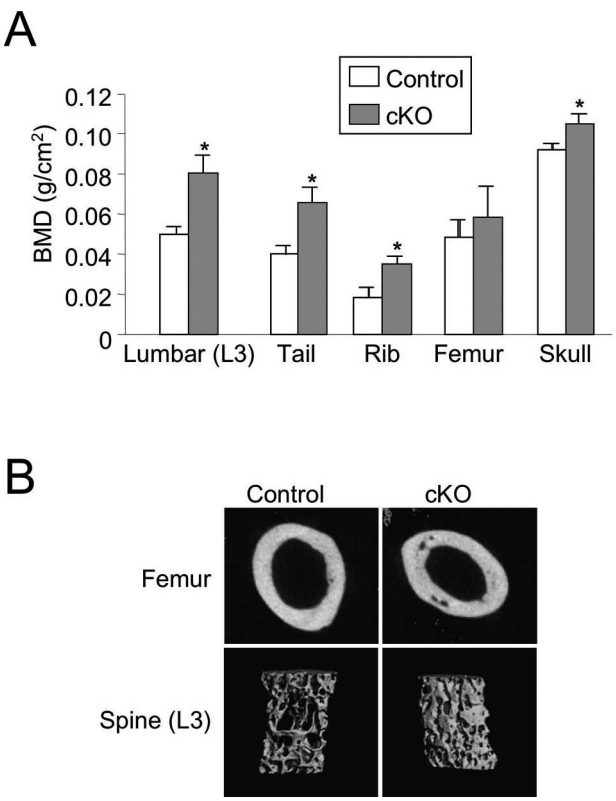

FIG. 4. Increased bone mass in cKO bones at 22 wk. (A) BMD was determined by DXA using lumbar (L_3), tails, ribs, femora, and skulls. Values are expressed as mean ± SD (control, $n = 8$; cKO, $n = 10$). *Statistically significant difference between control and cKO (mean ± SD, *t*-test; $*p < 0.01$). (B) Reconstructions of bone structure from μCT. Cortical bone in femora and trabecular bone in lumbar vertebrae (L_3) are shown. Trabecular bone was dramatically increased in cKO vertebrae (L_3).

suggest that a decrease in BMPRIA signaling may be leading toward a "trabecularization" of cortical bone. Taken together, P21 and 22-wk data suggest that *Bmpr1a* deficiency in osteoblasts increased bone mass mainly by increasing trabecular bone during both modeling and remodeling phases with some variation by site.

Reduced bone formation and resorption in Bmpr1a cKO bones

Bone mass is determined by the balance between formation and resorption. To further study the trabecular bone phenotype in cKO mice, these two factors were measured by static and dynamic histomorphometry. We chose 22-wk trabecular bones in femora and vertebrae because peak bone mass and strength in the mouse are achieved after 20 wk, with dynamic changes in both material and geometric properties.[10] Dynamic analysis showed a reduction of bone formation (BFR/BS) and mineral apposition rate (MAR) in trabecular bone of cKO femora (Fig. 5A). Dye deposition showed double lines in trabecular bone of control femora but did not in cKO (Fig. 5B). No significant decrease of N.Oc/T.Ar was observed in the femora trabeculae (control: 123.1 ± 30.8, cKO: 119.1 ± 15.6). Bone volume (BV/TV) and trabecular thickness (Tb.Th) were more increased in cKO vertebrae than femora by static bone histomorphometry (data not shown), consistent with the results from μCT analysis (Table 1). Osteoclast number per bone area (N.Oc/T.Ar) as determined by static analysis with TRACP staining was significantly reduced in vertebrae (L_3) of cKO mice (Fig. 5C). These results suggest that both bone formation and resorption were reduced by loss of BMPRIA signaling with some variation by site.

We next examined formation and resorption by measuring expression and serum levels of markers. RNA was extracted from weanling (P14) or adult (10–12 wk) mice (Figs. 1B and 1C). In adult vertebrae, expression levels of formation markers, *Runx2* (*Cbfa1*) and *Bsp,* were significantly reduced by ~60% (Fig. 6A), and resorption markers *Mmp9*, *Ctsk*, and *Tracp* were all significantly reduced >50% (Fig. 6B), consistent with the reduction in osteoclast number stained by TRACP (Fig. 5C). However, formation markers *Sp7* (osterix) and *Akp2* (alkaline phosphatase) were unchanged. Similar results were obtained from femora at this stage (data not shown). In weanling ribs where increased radiodensity was observed (Fig. 2A, a), bone formation markers were unchanged significantly (data not shown); however, *Tracp* significantly decreased by 40% (Fig. 6D). Osteoblasts regulate osteoclastogenesis by producing RANKL, an osteoclast differentiation factor, and osteoprotegerin (OPG), a decoy receptor for RANKL.[17–19] During adult stages, the expression of *Rankl* and *Opg* were significantly decreased and increased, respectively (Fig. 6C), resulting in a significant reduction of the ratio of *Rankl* to *Opg* by 70% (Fig. 6C). Similar results were obtained from weanling stages, beause the expression of *Opg* significantly increased by 50%, and the ratio of *Rankl* to *Opg* significantly decreased by 35% (Fig. 6D). Because RANKL stimulates osteoclastogenesis, whereas OPG inhibits it, these results suggest that osteoclastogenesis is decreased both in weanling and adult stages. Serum levels of the formation marker osteocalcin were significantly increased in adult cKO mice (data not shown), consistent with dramatically increased radiodensity at 22 wk (Fig. 2B). On the other hand, the resorption marker pyridinoline, RANKL, and the ratio of RANKL/OPG were nonsignificantly reduced in older mice (data not shown), partly because TM administration confounds straightforward interpretation of serum markers. It is also possible that timing of collecting serum is crucial for monitoring biological changes, because expression levels of resorption markers, *Rankl*, and *Opg* changed at earlier stages (10–12 weeks). Overall data suggest that resorption markedly decreases in cKO bones even though formation is somewhat reduced or unchanged, resulting in a net increase in bone mass.

To confirm the effect of BMP signaling on osteoclastogenesis through the RANKL–OPG pathway observed both in weanling and adult stages, we next set up a tissue culture system using newborn calvaria. Untreated cKO calvarial bones were collected from newborn mice (Cre^+, *Bmpr1afx/fx*), bisected, and cultured with or without 4-OH TM (100 ng/ml). Cre-dependent DNA recombination using this method was confirmed by β-gal staining of calvarial bones from *R26R* mice (Fig. 7A), and expression of *Bmpr1a* was

TABLE 1. TRABECULAR BONE MEASUREMENT BY μCT

	Spine (L_3)		*Femora*	
Parameters (unit)	*Control*	*cKO*	*Control*	*cKO*
BVF (BV/TV) (%)	35.7 ± 12.6	67.9 ± 14.5*	49.0 ± 15.8	59.7 ± 8.6
Trabecular thickness (mm)	61.9 ± 7.0	126.4 ± 52.2*	80.9 ± 13.1	108.3 ± 16.6*
Trabecular number (1/mm)	5.0 ± 0.9	6.9 ± 0.6*	6.8 ± 1.4	6.9 ± 1.0
Trabecular spacing (mm)	215.9 ± 38.7	124.4 ± 17.9*	129.3 ± 24.7	116.3 ± 31.5
Connectivity density (1/mm^3)	250.2 ± 75.0	169.3 ± 83.7†	232.7 ± 71.5	177.7 ± 49.0
Apparent density (mg/cm^3 HA)	402.9 ± 107.3	750.0 ± 159.1*	561.6 ± 135.3	675.4 ± 79.5
Tissue density (mg/cm^3 HA)	1041.9 ± 51.6	1093.7 ± 29.2†	1066.4 ± 30.1	1109.8 ± 24.3†

Data are mean ± SD; $n = 7$ (control); $n = 10$ (cKO). Significant differences are indicated between control and cKO (Student's t-test, *$p < 0.005$; $^\dagger p < 0.05$).

BVF, bone volume fraction (%); BV, trabecular bone volume (mm^3); TV, total volume selected for analysis (mm^3); HA, hydroxyapatite.

significantly reduced 78% in cKO (*Cre*$^+$, *Bmpr1afx/fx*, TM$^+$) compared with controls (*Cre*$^+$, *Bmpr1afx/fx*, TM$^-$; Fig. 7B). Expression levels of resorption markers *Mmp9*, *Ctsk*, and *Tracp* were significantly reduced >60% in cKO compared with controls (Fig. 7C). *Rankl* expression was reduced 41%, and *Opg* was significantly increased 12%, resulting in a 50% reduction of the ratio of *Rankl* to *Opg* in the treated group, which was significant (Fig. 7D). There were no significant differences in these expression levels between TM-treated (Cre$^-$, Bmpr1afx/fx, TM$^+$) and non-treated Cre negative bone (Cre$^-$, *Bmpr1a*fx/fx, TM$^-$) using littermate controls (data not shown). These results suggest that *Bmpr1a*-deficient osteoblasts reduced osteoclastogenesis through the RANKL–OPG pathway ex vivo, which corroborates in vivo results.

TABLE 2. CORTICAL BONE (FEMUR) MEASUREMENT BY μCT

Parameters (unit)	*Control*	*cKO*
Subperiosteal area (mm^2)	1.95 ± 0.44	1.73 ± 0.22
Subendosteal area (mm^2)	0.73 ± 0.22	0.64 ± 0.12
Segmented bone area (mm^2)	1.18 ± 0.22	1.04 ± 0.12
Periosteal perimeter (mm)	5.09 ± 0.54	4.84 ± 0.34
Endosteal perimeter (mm)	3.15 ± 0.45	2.99 ± 0.36
Cortical porosity (%)	0.033 ± 0.01	0.05 ± 0.02
Cortical thickness (mm)	0.31 ± 0.02	0.29 ± 0.03
Apparent density (mg/cm^3 HA)	1328.0 ± 15.0	1275.4 ± 34.4*
Tissue density (mg/cm^3 HA)	1490.46 ± 19.83	1457.67 ± 28.63†

Data are mean ± SD; $n = 7$ (Control); $n = 10$ (cKO). Significant differences are indicated between control and cKO (Student's t-test, *$p < 0.005$; $^\dagger p < 0.05$).

HA, hydroxyapatite.

DISCUSSION

Osteoblasts, BMP signaling, and bone mass

By using a 3.2-kb mouse procollagen *α1(I)* promoter,[9] we showed that reduction in BMP signaling through BMPRIA in osteoblasts increased bone mass both in P21 and 22-wk mice. We also observed increased bone mass in another conditional *Bmpr1a* knockout mouse (data not shown) using *Col13.6-Cre* mice.[20] These bone phenotypes are consistent with our previous report that showed increased bone volume (BV/TV) at 10 mo by loss of BMP signaling in osteoblasts using *Og2-Cre* mice, but it is not consistent with the 3-mo mice, which showed decreased bone mass.[8] The bone phenotype observed in *Bmpr1a*-deficient mice with *Og2-Cre*[8] was milder than that with *Col1-CreER^{TM}*. These discrepancies may be caused by differences in the timing of recombination between promoters. Aubin[21] described characteristics of osteoblasts that change along with their maturation; thus, the effects of disrupting BMPRIA signaling may be influenced by the stages of osteoblastic maturation. In *Col1-CreER^{TM}* mice, Cre activity was detected in immature periosteum wrapping growth plates, in osteogenic centers, and in bone collars during embryonic stages (data not shown). Therefore, *Col1-CreER^{TM}* mice can induce recombination earlier in osteoblastogenesis, including in pre-osteoblasts, compared with *Og2-Cre* mice, which could explain why the *Bmpr1a*-deficient mice using *Og2-Cre* mice did not change expression levels of early osteogenic markers *Runx2* and *Bsp*.[8] These in vivo experiments taken together support in vitro evidence[21] and imply that the response of osteoblasts to BMP signaling differs both by age and differentiation stage. Further studies of embryonic and older mice using *Col1-CreER^{TM}* mice and comparisons of the bone phenotype in *Bmpr1a* deficiency among different osteoblast-specific Cre mice are desired to address the diverse function of BMP signaling.

BMP signaling and osteoclastogenesis

Mouse genetic models using BMP ligands and antagonists instead of receptors were recently reported. Overexpression of *Bmp4* in osteoblasts reduced bone mass at E18.5 with upregulation of osteoclastogenesis.[22] Overexpression of *Noggin*, an antagonist of BMP2 and BMP4, in osteoblasts increased bone mass with reduced osteoclast number (N.Oc/BS) and osteoclastogenesis both at E17.5 and 3 wk.[22] These studies are consistent with our findings, because BMP2 and BMP4 are potent agonists of BMPRIA. Taken together with our results, these studies suggest that BMP signaling in osteoblasts negatively regulates bone mass by upregulating osteoclastogenesis.

Reduction in osteoclast number (Fig. 5C) and expression levels of functional markers (*Mmp9*, *Ctsk*, and *Tracp*) (Fig. 6B) showed downregulated osteoclastogenesis in cKO mice, which may direct rib flaring (Fig. 2). The reduction of

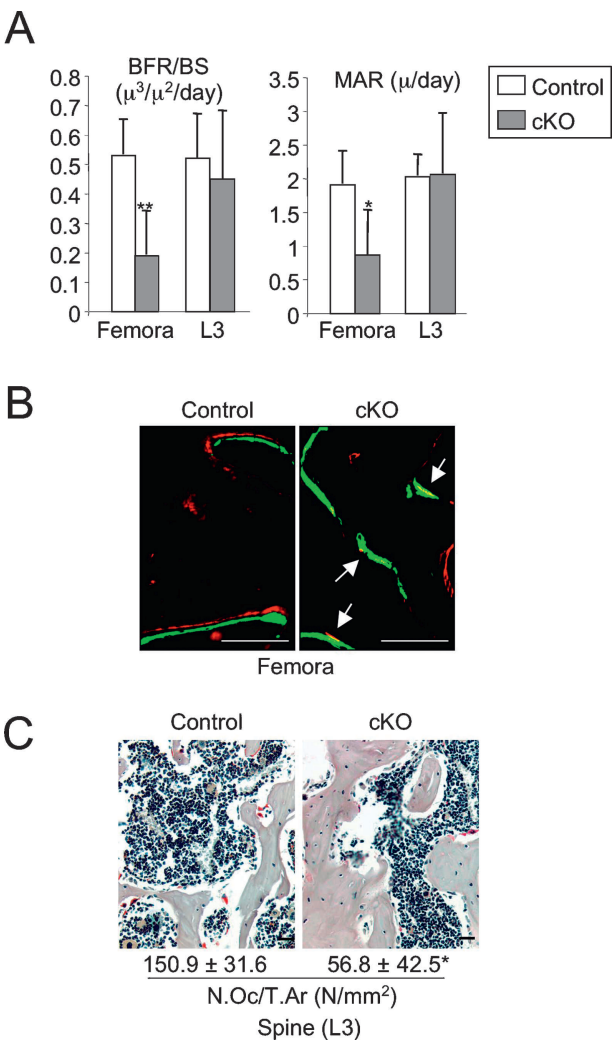

FIG. 5. Morphometric markers for bone formation and resorption at 22 wk. (A) Dynamic (BFR/BS and MAR) analyses were performed using trabecular bone of femora and lumbar vertebrae (L_3) from control ($n = 10$) and cKO ($n = 10$) mice. *Statistically significant difference between control and cKO (*t*-test; $*p < 0.05$; $**p < 0.005$; BFR/BS, bone formation rate over bone surface; MAR, mineral apposition rate). (B) Dynamic histomorphometric analysis of cKO bones by double label staining of trabecular bone in femora with calcein and xylenol orange. Dotted and random staining pattern was shown in cKO. White arrows indicate merging of double labeled staining in cKO bone. Bars: 100 μm. (C) Static histomorphometric analysis of L_3 trabecular bone with TRACP staining. Values are expressed as mean ± SD (control, $n = 5$; cKO, $n = 5$). *Statistically significant difference between control and cKO (mean ± SD, *t*-test; $*p < 0.05$). N.Oc/T.Ar, osteoclast number per bone area. Bars: 100 μm.

osteoclastogenesis in cKO mice is presumably caused by the defect in osteoblasts, because the 3.2-kb type I collagen promoter directed Cre recombination in osteoblasts but not osteoclasts (Fig. 1F). Osteoblasts regulate osteoclast by expressing RANKL, an osteoclast differentiation factor, and OPG, a decoy receptor for RANKL.[17–19] The link between BMP signaling and the RANKL–OPG pathway has not been studied in vivo, because this signaling was unchanged in mice overexpressing *Noggin* or *Bmp4* in osteoblasts using the 2.3-kb type I collagen promoter[22] and knocking out BMPRIA using osteocalcin promoter (*Og2-Cre* mice).[8] This study is the first in vivo evidence showing that loss of BMP signaling reduces osteoclastogenesis by downregulating RANKL and upregulating OPG. Because the 2.3-kb type I collagen and osteocalcin promoter are first activated in mature osteoblasts,[20,23] it is possible that immature osteoblastic stages, where the 3.2-kb type I collagen promoter is active, are crucial for regulating osteoclastogenesis through the RANKL–OPG pathway.

BMP signaling, bone formation, and mineralization

Bone formation rate (BFR/BS) in femoral trabecular bone was reduced in 22-wk mice by loss of function of BMPRIA in osteoblasts (Fig. 5A), consistent with the previous report.[8] Overexpression of *Noggin* in osteoblasts also reduced the formation rate at P21.[22] These facts suggest that BMP signaling is critical for bone formation in vivo, which supports in vitro evidence that BMPs induce osteogenesis. However, in *Bmpr1a* cKO mice, the reduction of formation rate in femora was more severe than that in vertebrae, and mineral apposition rate (MAR) was reduced in femora but not in vertebrae. These results suggest that the effect BMP signaling has on bone formation may differ in a site-specific manner in vivo, which can explain variations in changes in BMD and volume in cKO bones as determined by X-ray, DXA, and μCT. Further study is necessary to understand the mechanism of the site specificity in vivo, which would be difficult to assess in vitro.

In addition, changes noted in the cortices were not consistent with findings in the trabeculae. One of the major contextual differences that could contribute to the unique osteotropic response to BMP signaling in the trabeculae compared with other sites such as cortical bone, perichondrium, and skeletal muscle (ectopic) is the immediate juxtaposition of trabecular osteoblasts to the hematopoietic lineage. The 3.2-kb promoter used in *Col1-CreER^{TM}* mice is active in pre-osteoblasts, osteoblasts, periosteum, and osteocytes widely throughout all bones examined. Site-specific promoters for Cre recombination could be developed to answer these questions.

BMD as determined by X-ray, DXA, and μCT was increased in cKO ribs, vertebrae, and tails at 22 wk (Figs. 2–4). These results indicate that loss of BMP signaling enhances bone mineralization. Interestingly, two in vitro studies have data that support our findings. One showed an increase in mineralization by overexpressing truncated BMPRIA without a kinase domain to block BMP signaling.[24] Another showed an inhibition of mineralization by adding exogenous BMP2 into culture.[25] Neither interpreted these results in their discussions. However, these facts suggest that BMP signaling negatively regulates mineralization in vivo. Another possibility is that loss of BMPRIA signaling causes a decrease in bone resorption. The existing matrix ages and continues to mineralize, similar to the proposed mechanism for the increase in BMD observed in humans on bisphosphonate therapy.[26,27] In addition, serum levels of osteocalcin increased (data not shown), indicating an increased number of osteoblast and

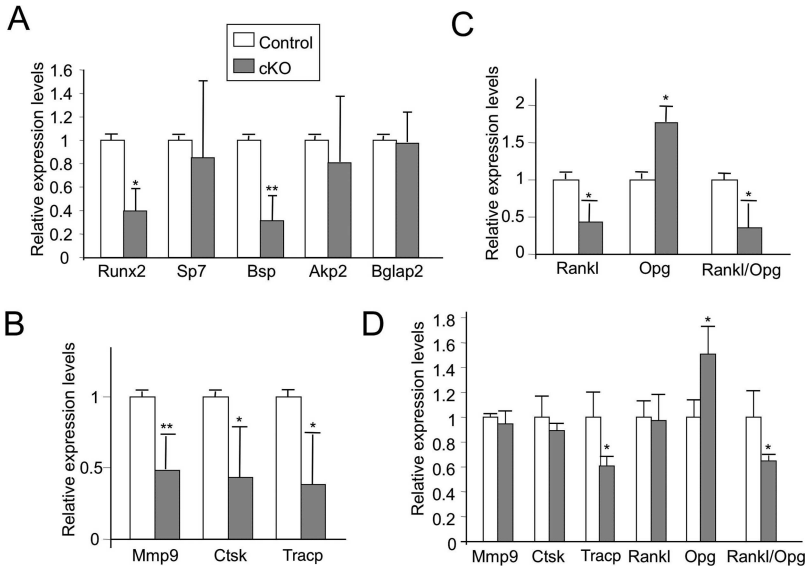

FIG. 6. Expression levels of bone formation and resorption markers during adult and weanling stages. RNA was extracted from vertebrae of 10- to 12-wk mice for adult stages and ribs of P14 for weanling stages. (A) Quantitative RT-PCR for bone formation markers (*Runx2*, *Sp7*, *Bsp*, *Akp2*, and *Bglap2*) during adult stages. Expression levels of both *Runx2* and *Bsp* were significantly reduced in cKO. (B) Quantitative RT-PCR for bone resorption markers expressed by osteoclasts (*Mmp9*, *Ctsk*, and *Tracp*) during adult stages. These expression levels were all reduced over 50% in cKO. (C) Quantitative RT-PCR for *Opg* and *Rankl* expressed by osteoblasts and relative ratio of *Rankl* to *Opg* expression levels during adult stages. The expression of *Rankl* was significantly reduced by 60%, and *Opg* was significantly increased by 80%, resulting in a significant reduction in the ratio of *Rankl* to *Opg* by 70% in cKO. (D) Quantitative RT-PCR for bone resorption markers (*Mmp9*, *Ctsk*, and *Tracp*) and RANKL–OPG pathway (*Opg* and *Rankl*), and relative ratio of *Rankl* to *Opg* expression levels during weanling stages. The expression of *Tracp* decreased by 40% and *Opg* increased by 50%, both significantly. The ratio of *Rankl* to *Opg* expression levels significantly decreased 35%. Similar results were obtained from femora during adult stages. *Statistically significant difference between cKO and control from three independent experiments in A–D (mean ± SD, *t*-test; $*p < 0.05$; $**p < 0.001$).

osteocytes, which is consistent with increased bone mass in *Bmpr1a* cKO mice. This fact may also contribute to increased mineralization in cKO bones. Further study is necessary to address the mechanism by which BMP signaling controls bone mineralization.

BMP signaling, endogenous bone, and ectopic bone

Osteoblasts and chondrocytes both affect bone mass and are the predominant cell types in bone and cartilage, respectively. However, the difference in molecular mechanisms by which BMP signaling regulates these cell types to control bone mass is largely unknown, partly because of a lack of appropriate mouse genetic models. In this study, we found that osteoblasts lacking *Bmpr1a* fail to support osteoclastogenesis, leading to an increase in endogenous bone mass. Thus, we propose that BMP signaling in osteoblasts has dual functions to balance bone mass; it enhances bone formation by osteoblasts and enhances bone resorption by supporting osteoclastogenesis. However, studies focusing on BMP receptors in chondrocytes suggest that these cells respond to BMP signaling by increasing bone mass during the endochondral formation process.[15,28] Mice overexpressing *Bmp4* in mesenchymal cells and chondrocytes increase bone mass, whereas overexpression of *Noggin* in those cells decreases bone mass.[22,29] In addition, recent mouse studies in which Cre expression is driven by a promoter in mesenchymal cells and chondrocytes (*Prx1-Cre*)[30,31] showed that the disruption of BMP ligands in these cells impaired osteogenesis, resulting in reduced bone mass, and blocked fracture healing, which follows endochondral bone formation. Taken together, we propose that BMP signaling in chondrocytes increases bone mass but BMP signaling in osteoblasts restrains endogenous bone mass.

BMPs given subcutaneously induce ectopic bone formation.[1] Human genetics showed that enhanced BMP signaling by a point mutation in *ACVR1*, another BMP type I receptor, causes fibrodysplasia ossificans progressiva (FOP) with ectopic bones in muscle.[32] These ectopic bones in muscle may form primarily because of the effect of BMP signaling on chondrocytes as we discussed above, because ectopic bone formation follows an endochondral formation pattern. The FDA approved BMP2 and BMP7 for clinical use to improve fracture healing.[33] However, our finding of increased bone mass by loss of BMPRIA is unexpected and contrary to the rationale behind clinical applications of BMPs in orthopedics. Current clinical data supporting their use is underdeveloped[3,4]; this may be in part because of a lack of understanding of the variable effects BMPs have on different cell types in the skeleton including chondrocytes, osteoblasts, and osteoclasts. In addition, species differences might also play a role in the lack of efficacy in human clinical trials. Whereas much of the in vitro and in vivo analyses have been done on mouse cells and mouse models, demonstration of the effects of BMPs on human cells in vitro are modest because of species differences.[34]

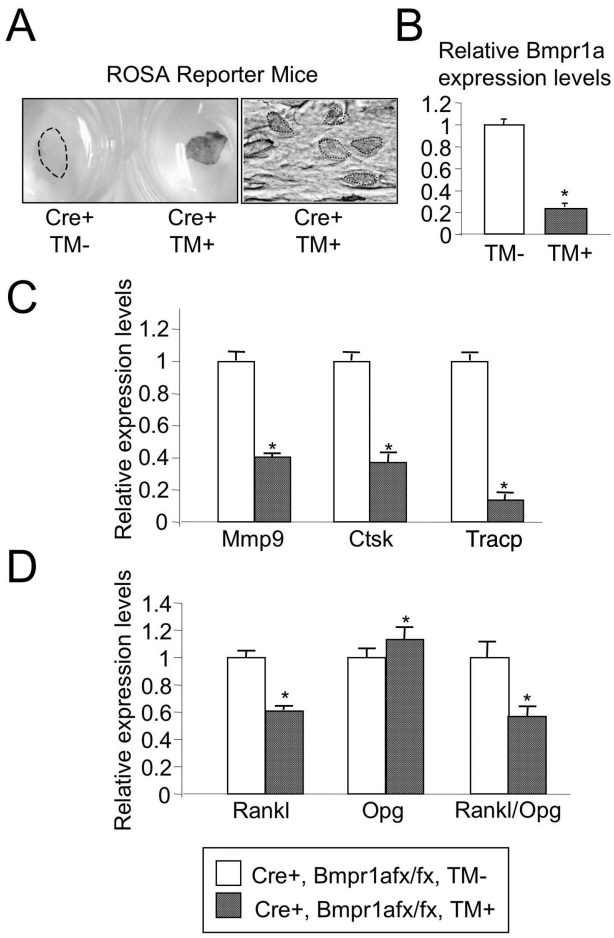

FIG. 7. Reduced osteoclastogenesis by loss of BMPRIA ex vivo. (A) Cre activity was assessed using *R26R*. When Cre-positive calvarial bones from newborn mice were treated with 4-hydroxyl TM (100 ng/ml) for 5 days, Cre-dependent DNA recombination was detected by β-gal staining (Cre^+, TM^+) compared with no staining in untreated bones (Cre^+, TM^-). Histological analysis showed that osteoblasts were positive for β-gal. Stained nuclei were circled with dotted line. (B) Quantitative RT-PCR for *Bmpr1a* using calvarial bones (Cre^+, Bmpr1afx/fx) with or without 4-hydroxyl TM. Calvarial bones were collected from newborn mice, which did not receive TM before death. *Bmpr1a* expression was significantly reduced after TM treatment (TM^+) compared with nontreated (TM^-). (C) Quantitative RT-PCR for bone resorption markers expressed by osteoclasts (*Mmp9*, *Ctsk*, and *Tracp*). (D) Quantitative RT-PCR for *Opg* and *Rankl* expressed by osteoblasts, and relative ratio of *Rankl* to *Opg* expression levels. There were no significant differences in these expression levels between TM-treated (*Cre*$^-$, *Bmpr1afx/fx*, TM^+) and nontreated (*Cre*$^-$, *Bmpr1afx/fx*, TM^-) bones using littermate controls (data not shown). *Statistically significant difference between TM^+ and TM^- from three independent experiments in B–D (mean ± SD, *t*-test; $*p < 0.05$).

Future work will focus on the mechanisms by which loss of BMPRIA signaling in osteoblasts impacts remodeling. This may best be performed in older animals, perhaps challenged with ovariectomy, orchiectomy, fracture, or immobilization.

In conclusion, this study shows that loss of BMP signaling by BMPRIA directs osteoblasts to increase bone mass primarily in trabecular bone in part by downregulating osteoclastogenesis through the RANKL–OPG pathway. In osteoblasts, BMPRIA is a signaling molecule that directs both bone formation and resorption to reduce endogenous bone mass in vivo.

ACKNOWLEDGMENTS

We thank Dr Douglas J Adams for μCT measurement, Dr Gloria A Gronowicz and Felicia Ledgard for bone histomorphometry, Toni Ward for mouse dosing, Gregory Travlos and Bridget Garner for serum biochemistry, and Naomasa Keiko, Mikiko Kamiya, and Dr Katsuji Shimizu for encouragement. This work was supported by NIH Grants P01 DK56246 (to HK), R01 AR051587 (to JF), R21 AR052824 (to MY), and the Intramural Research Program of the NIEHS, NIH (to YM, ES071003-10). The NIEHS Fellowship in Environmental Medicine supported DL. The Lilly Fellowship Foundation supported NK.

REFERENCES

1. Urist MR 1965 Bone: Formation by autoinduction. Science **150:**893–899.
2. Chen D, Zhao M, Mundy GR 2004 Bone morphogenetic proteins. Growth Factors **22:**233–241.
3. Wingerter S, Tucci M, Bumgardner J, Benghuzzi H 2007 Evaluation of short-term healing following sustained delivery of osteoinductive agents in a rat femur drill defect model. Biomed Sci Instrum **43:**188–193.
4. Gautschi OP, Frey SP, Zellweger R 2007 Bone morphogenetic proteins in clinical applications. ANZ J Surg **77:**626–631.
5. Zhang H, Bradley A 1996 Mice deficient for BMP2 are nonviable and have defects in amnion/chorion and cardiac development. Development **122:**2977–2986.
6. Winnier G, Blessing M, Labosky PA, Hogan BL 1995 Bone morphogenetic protein-4 is required for mesoderm formation and patterning in the mouse. Genes Dev **9:**2105–2116.
7. Mishina Y, Suzuki A, Ueno N, Behringer RR 1995 Bmpr encodes a type I bone morphogenetic protein receptor that is essential for gastrulation during mouse embryogenesis. Genes Dev **9:**3027–3037.
8. Mishina Y, Starbuck MW, Gentile MA, Fukuda T, Kasparcova V, Seedor JG, Hanks MC, Amling M, Pinero GJ, Harada S, Behringer RR 2004 Bone morphogenetic protein type IA receptor signaling regulates postnatal osteoblast function and bone remodeling. J Biol Chem **279:**27560–27566.
9. Rossert J, Eberspaecher H, de Crombrugghe B 1995 Separate cis-acting DNA elements of the mouse pro-alpha 1(I) collagen promoter direct expression of reporter genes to different type I collagen-producing cells in transgenic mice. J Cell Biol **129:**1421–1432.
10. Brodt MD, Ellis CB, Silva MJ 1999 Growing C57Bl/6 mice increase whole bone mechanical properties by increasing geometric and material properties. J Bone Miner Res **14:**2159–2166.
11. Hayashi S, McMahon AP 2002 Efficient recombination in diverse tissues by a tamoxifen-inducible form of Cre: A tool for temporally regulated gene activation/inactivation in the mouse. Dev Biol **244:**305–318.
12. Danielian PS, Muccino D, Rowitch DH, Michael SK, McMahon AP 1998 Modification of gene activity in mouse embryos in utero by a tamoxifen-inducible form of Cre recombinase. Curr Biol **8:**1323–1326.
13. Mishina Y, Hanks MC, Miura S, Tallquist MD, Behringer RR 2002 Generation of Bmpr/Alk3 conditional knockout mice. Genesis **32:**69–72.
14. Soriano P 1999 Generalized lacZ expression with the ROSA26 Cre reporter strain. Nat Genet **21:**70–71.

15. Yoon BS, Ovchinnikov DA, Yoshii I, Mishina Y, Behringer RR, Lyons KM 2005 Bmpr1a and Bmpr1b have overlapping functions and are essential for chondrogenesis in vivo. Proc Natl Acad Sci USA **102:**5062–5067.
16. Livak KJ, Schmittgen TD 2001 Analysis of relative gene expression data using real-time quantitative PCR and the 2(-Delta Delta C(T)) method. Methods **25:**402–408.
17. Lacey DL, Timms E, Tan HL, Kelley MJ, Dunstan CR, Burgess T, Elliott R, Colombero A, Elliott G, Scully S, Hsu H, Sullivan J, Hawkins N, Davy E, Capparelli C, Eli A, Qian YX, Kaufman S, Sarosi I, Shalhoub V, Senaldi G, Guo J, Delaney J, Boyle WJ 1998 Osteoprotegerin ligand is a cytokine that regulates osteoclast differentiation and activation. Cell **93:**165–176.
18. Simonet WS, Lacey DL, Dunstan CR, Kelley M, Chang MS, Luthy R, Nguyen HQ, Wooden S, Bennett L, Boone T, Shimamoto G, DeRose M, Elliott R, Colombero A, Tan HL, Trail G, Sullivan J, Davy E, Bucay N, Renshaw-Gegg L, Hughes TM, Hill D, Pattison W, Campbell P, Sander S, Van G, Tarpley J, Derby P, Lee R, Boyle WJ 1997 Osteoprotegerin: A novel secreted protein involved in the regulation of bone density. Cell **89:**309–319.
19. Yasuda H, Shima N, Nakagawa N, Mochizuki SI, Yano K, Fujise N, Sato Y, Goto M, Yamaguchi K, Kuriyama M, Kanno T, Murakami A, Tsuda E, Morinaga T, Higashio K 1998 Identity of osteoclastogenesis inhibitory factor (OCIF) and osteoprotegerin (OPG): A mechanism by which OPG/OCIF inhibits osteoclastogenesis in vitro. Endocrinology **139:**1329–1337.
20. Kalajzic I, Kalajzic Z, Kaliterna M, Gronowicz G, Clark SH, Lichtler AC, Rowe D 2002 Use of type I collagen green fluorescent protein transgenes to identify subpopulations of cells at different stages of the osteoblast lineage. J Bone Miner Res **17:**15–25.
21. Aubin JE 1998 Advances in the osteoblast lineage. Biochem Cell Biol **76:**899–910.
22. Okamoto M, Murai J, Yoshikawa H, Tsumaki N 2006 Bone morphogenetic proteins in bone stimulate osteoclasts and osteoblasts during bone development. J Bone Miner Res **21:**1022–1033.
23. Ducy P, Karsenty G 1995 Two distinct osteoblast-specific cis-acting elements control expression of a mouse osteocalcin gene. Mol Cell Biol **15:**1858–1869.
24. Chen D, Ji X, Harris MA, Feng JQ, Karsenty G, Celeste AJ, Rosen V, Mundy GR, Harris SE 1998 Differential roles for bone morphogenetic protein (BMP) receptor type IB and IA in differentiation and specification of mesenchymal precursor cells to osteoblast and adipocyte lineages. J Cell Biol **142:**295–305.
25. Luppen CA, Smith E, Spevak L, Boskey AL, Frenkel B 2003 Bone morphogenetic protein-2 restores mineralization in glucocorticoid-inhibited MC3T3-E1 osteoblast cultures. J Bone Miner Res **18:**1186–1197.
26. Boivin GY, Chavassieux PM, Santora AC, Yates J, Meunier PJ 2000 Alendronate increases bone strength by increasing the mean degree of mineralization of bone tissue in osteoporotic women. Bone **27:**687–694.
27. Chapurlat RD, Delmas PD 2006 Drug insight: Bisphosphonates for postmenopausal osteoporosis. Nat Clin Pract Endocrinol Metab **2:**211–219.
28. Rountree RB, Schoor M, Chen H, Marks ME, Harley V, Mishina Y, Kingsley DM 2004 BMP receptor signaling is required for postnatal maintenance of articular cartilage. PLoS Biol **2:**e355.
29. Tsumaki N, Nakase T, Miyaji T, Kakiuchi M, Kimura T, Ochi T, Yoshikawa H 2002 Bone morphogenetic protein signals are required for cartilage formation and differently regulate joint development during skeletogenesis. J Bone Miner Res **17:**898–906.
30. Bandyopadhyay A, Tsuji K, Cox K, Harfe BD, Rosen V, Tabin CJ 2006 Genetic Analysis of the Roles of BMP2, BMP4, and BMP7 in Limb Patterning and Skeletogenesis. PLoS Genet **2:**e216.
31. Tsuji K, Bandyopadhyay A, Harfe BD, Cox K, Kakar S, Gerstenfeld L, Einhorn T, Tabin CJ, Rosen V 2006 BMP2 activity, although dispensable for bone formation, is required for the initiation of fracture healing. Nat Genet **38:**1424–1429.
32. Shore EM, Xu M, Feldman GJ, Fenstermacher DA, Cho TJ, Choi IH, Connor JM, Delai P, Glaser DL, LeMerrer M, Morhart R, Rogers JG, Smith R, Triffitt JT, Urtizberea JA, Zasloff M, Brown MA, Kaplan FS 2006 A recurrent mutation in the BMP type I receptor ACVR1 causes inherited and sporadic fibrodysplasia ossificans progressiva. Nat Genet **38:**525–527.
33. Simpson AH, Mills L, Noble B 2006 The role of growth factors and related agents in accelerating fracture healing. J Bone Joint Surg Br **88:**701–705.
34. Osyczka AM, Diefenderfer DL, Bhargave G, Leboy PS 2004 Different effects of BMP-2 on marrow stromal cells from human and rat bone. Cells Tissues Organs **176:**109–119.

Address reprint requests to:
Yuji Mishina, PhD
University of Michigan
School of Dentistry
Department of Biologic and Materials Sciences
4222A Dental
1011 North University Avenue
Ann Arbor, MI 48109-1078, USA
E-mail: mishina@umich.edu

Received in original form February 26, 2008; revised form May 29, 2008; accepted July 31, 2008.